

Supporting Information
for
Degradation-Resistant Trehalose Analogues Block Utilization of Trehalose by
Hypervirulent *Clostridioides difficile*

Noah D. Danielson,^{a,†} James Collins,^{b,†} Alicyn I. Stothard,^a Qing Qing Dong,^a Karishma Kalera,^a Peter J.
Woodruff,^c Brian J. DeBosch,^{d,e} Robert A. Britton,^b and Benjamin M. Swarts^{*,a}

^a Department of Chemistry and Biochemistry, Central Michigan University, Mount Pleasant, MI, USA.

^b Baylor College of Medicine, Department of Molecular Virology and Microbiology, Houston, TX, USA

^c Department of Chemistry, University of Southern Maine, Portland, ME, USA

^d Department of Pediatrics, Washington University School of Medicine, St. Louis, MO, USA

^e Department of Cell Biology & Physiology, Washington University School of Medicine, St. Louis, MO,
USA

[†] These authors contributed equally to this work.

*Corresponding author. E-mail: ben.swarts@cmich.edu

Table of Contents

I. Supplementary Figures and Tables.....	S3
Figure S1. EXSIDE spectra of compounds 1–4	S3
Table S1. Glycosidic dihedral angles of compounds 1–4	S3
Figure S2. Dependence of mannotrehalose-supported RT027 growth on TreA.....	S4
Figure S3. 5-Thiotrehalose activity against RT078 is specific for trehalose metabolism.....	S4
Table S2. Cytotoxicity of 5-thiotrehalose in HEK 293 cells	S5
Figure S4. Effect of Validamycin A on <i>C. difficile</i> trehalose utilization.....	S5
II. Experimental Methods	S6
III. References.....	S9

I. Supplementary Figures and Tables

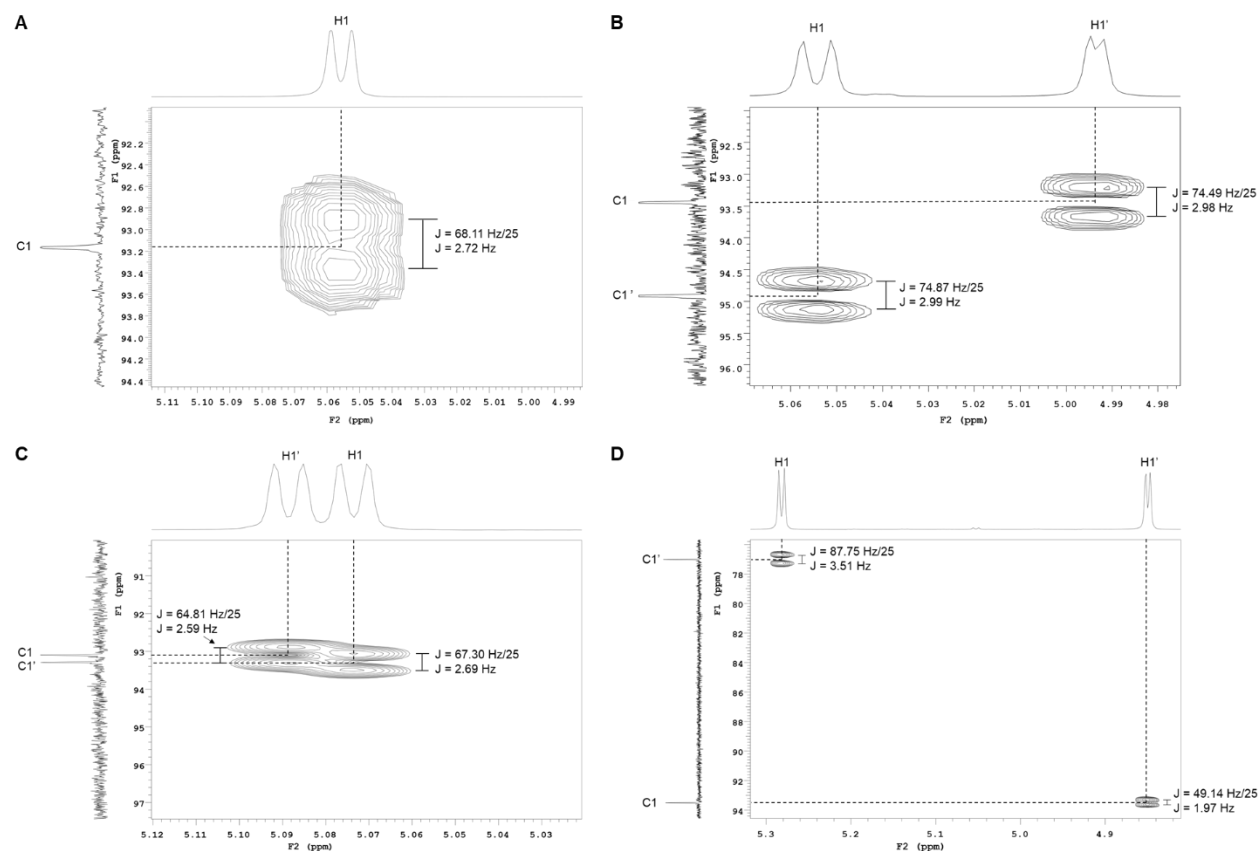


Figure S1. EXSIDE spectra showing long-range heteronuclear couplings across the glycosidic bond for (A) trehalose (**1**), (B) mannotrehalose (**2**), (C) lactotrehalose (**3**), and (D) 5-thiotrehalose (**4**). Dashed lines indicate cross-peaks between H1–C1' and H1'–C1 for each compound. $^3J_{\text{COCH}}$ constants were measured from EXSIDE spectra doublets using a scaling factor of 25, as shown.

Table S1. Glycosidic dihedral angles for trehalose and trehalase-resistant trehalose analogues.^a

Compound	φ_{H}^b ; $^3J_{\text{COCH}}$	ψ_{H}^b ; $^3J_{\text{COCH}}$
Trehalose (1)	–47.2°; 2.72 Hz	–47.2°; 2.72 Hz
Mannotrehalose (2)	–44.4°; 2.98 Hz	–44.3°; 2.99 Hz
Lactotrehalose (3)	–47.5°; 2.69 Hz	–48.6°; 2.59 Hz
5-Thiotrehalose (4)	–38.6°; 3.51 Hz	–55.8°; 1.97 Hz

^a Only NMR-determined values are shown.

^b Calculated using the Karplus equation of Tvaroška (Eq. 1).¹

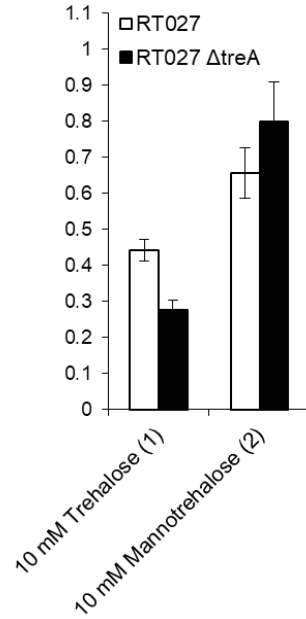


Figure S2. Growth of *C. difficile* RT027 on mannotrehalose is not dependent on the phosphotrehalase TreA. The indicated strains were grown in DMM containing the indicated carbon source and growth was assessed by monitoring OD₆₀₀ over 16 h. Error bars represent the standard deviation from three biological replicates.

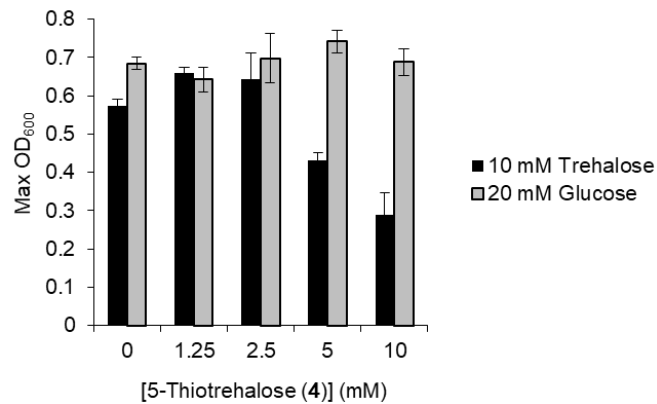


Figure S3. 5-Thiotrehalose blocks growth of *C. difficile* RT078 on trehalose but not glucose. RT078 was grown in DMM containing the indicated carbon source and concentration of 5-thiotrehalose, and growth was assessed by monitoring OD₆₀₀ over 16 h. Error bars represent the standard deviation from three biological replicates.

Table S2. Cytotoxicity analysis of 5-thiotrehalose against HEK 293 cells.^a

[5-Thiotrehalose (4)] (mM)	OD ₄₉₀	% Cytotoxicity
0	0.191 ± 0.002	N/A
2.5	0.147 ± 0.002	−32.7
5.0	0.163 ± 0.005	−19.5
10	0.165 ± 0.005	−17.7
Spontaneous LDH activity (negative control)	0.186 ± 0.008	N/A
Maximum LDH activity (positive control)	0.305 ± 0.040	N/A

^aData obtained using a commercially available LDH cytotoxicity assay kit (Pierce).

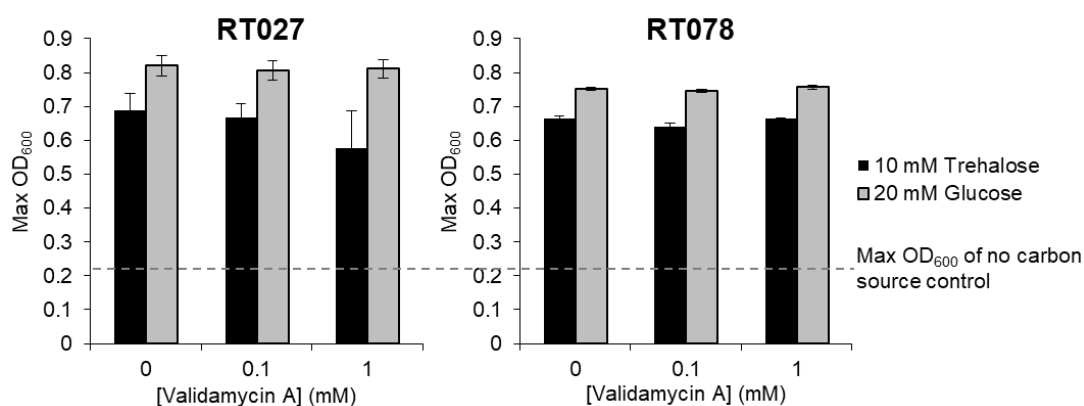


Figure S4. Validamycin A (0.1–1 mM) does not affect growth of *C. difficile* RT078 or RT028 on trehalose or glucose. RT078 and RT027 were grown in DMM containing the indicated carbon source and concentration of Validamycin A, and growth was assessed by monitoring OD₆₀₀ overnight. Error bars represent the standard deviation from three biological replicates.

II. Experimental Procedures

Synthesis of trehalose analogues. TreT was expressed and purified from *E. coli* as previously described.^{2,3} UDP-Glucose was obtained from Abcam. Mannotrehalose (**2**) and 5-thiotrehalose (**4**) were chemoenzymatically synthesized from the corresponding glucose analogues and UDP-glucose using TreT catalysis as reported by Wolber *et al.*⁴ Lactotrehalose (**3**) was chemically synthesized as reported by Bassily *et al.*⁵ ¹H and ¹³C NMR spectra matched the literature data for all compounds, and purity of all compounds was determined by ¹H NMR to be $\geq 98\%$.

Conformational analysis of trehalose analogues. NMR and molecular modeling were performed essentially as described.² Briefly, Deuterium-exchanged trehalose and trehalose analogues were dissolved in D₂O (99.8%) to a final concentration of 100 mM. Argon was bubbled through the solution for 1 min and then the tube was sealed with parafilm. To obtain ¹H, ¹³C, COSY, and HSQC spectra, samples were analyzed on a Varian INOVA 500 and for EXSIDE, a 600 instrument at room temperature equipped with a 5-mm indirect PFG HCN probe was used. For HSQC spectra, in-phase cross-peaks correspond to CH/CH₃ carbons, cross-peaks with opposite phase correspond to CH₂ carbons. ¹H NMR spectra were referenced to residual HDO peak at δ 4.78 ppm. Standard Varian pulse sequences were used for 1D and 2D experiments. NMR data were processed, analyzed, and plotted using Varian VnmrJ version 4.2 revision A.

For experimental determination of ³J_{COCH} values, a Varian selexcit experiment with multifrequency excitation of the anomeric H1 and H1' protons was set up using a previously acquired 1D proton spectrum of the appropriate disaccharide. The selexcit experiment was used to configure a 2D excitation-sculptured indirect-detection NMR experiment (EXSIDE),⁶ which enabled the measurement of long-range heteronuclear coupling constants. Both the selexcit and EXSIDE experiments were part of the standard Varian VnmrJ software package. EXSIDE spectra were obtained using 4 scans in the F2 (¹H) dimension, 512 increments in the F1 dimension (¹³C), a jnxxh setting of 4, and a *J* scaling factor (*N*) of 25. Long-range couplings were observed as in-phase pairs in the F1 dimension of the 2D spectrum. ³J_{COCH} values were determined from the EXSIDE spectra using the following equation:

$$J = \frac{([\delta_2 - \delta_1] * 125.7 \text{ MHz})}{N}$$

where δ_2 and δ_1 are the chemical shifts of each cross-peak in a pair, 125.7 MHz is the ¹³C NMR frequency, and *N* is the *J* scaling factor 25. Next, the ³J_{COCH} values were converted into approximate dihedral angles using the Karplus equation developed by Tvaroška and co-workers¹:

$$J = 5.7\cos^2(\theta) - 0.6\cos^2(\theta) + 0.5$$

Molecular mechanics calculations employing the MM3* force field⁷ were used to predict the solution conformations of trehalose and trehalose analogues. All MM3* calculations were performed in MacroModel version 11.2 in the Maestro environment (version 10.5) running on the Windows 10 operating system. First, structures for trehalose and the analogues were built with the appropriate stereochemical configurations. The structures were energy-minimized with MM3* using the Polak-Ribiere Conjugate Gradient (PRCG) method and a maximum of 2500 iterations. Next, these structures were used to initiate conformational searches using the Monte Carlo Multiple Minimum (MCMM) torsional sampling algorithm on all rotatable bonds, including ring closure. 1000 structures were sampled using MCMM. All MM3* calculations were performed with water selected as the solvent. MCMM conformational searches were performed with glycosidic dihedral angle constraints determined experimentally by NMR as described above. The lowest-energy conformers were selected for visual depiction in the manuscript.

Resistance of analogues to porcine trehalase. To a 1.5 mL microcentrifuge tube was added 40 μ L phosphate-buffered saline (PBS) and 50 μ L of trehalose or trehalose analogue stock solution (20 mM) in PBS. Porcine kidney trehalase (Sigma Aldrich) was diluted 1:100 in PBS, and 10 μ L of this solution was added to the microcentrifuge tube. The final concentrations of the trehalose analogue and enzyme were 10 mM and \sim 0.8 μ g/mL, respectively, and the final reaction volume was 100 μ L. Control experiments lacking trehalase were run in parallel. After mixing the contents of the tube thoroughly, the tube was incubated at 37 °C with shaking for 8 h. At time points of 1 h, 2 h, 4 h, and 8 h, aliquots of the reactions were taken and treated with an equal volume of cold acetone to precipitate protein and centrifuged, then the supernatants were removed and analyzed by thin-layer chromatography (TLC). Using glass-backed silica 60 Å plates (thickness 250 μ m), the samples were spotted onto pre-marked positions along the bottom of the plate. Standards of hydrolysis products, either glucose (for trehalose) or glucose analogue (for the corresponding trehalose analogue), were also spotted onto the plates for comparison. The solutions were left to dry for 15–20 min, and then developed using 5:3:2 *n*-butanol:ethanol:water. The plates were dried for 15–20 min, then stained with 5% H₂SO₄ in ethanol and heated on a hot plate until all sugar-containing spots were clearly visualized.

Porcine trehalase inhibition assays. Inhibition of porcine trehalase by trehalose analogues was assessed using a commercially available trehalase assay kit (Megazyme). In this assay, trehalase-catalyzed breakdown of trehalose yields two moles of glucose, which are converted by hexokinase to glucose-6-phosphate (G6P), which in turn is oxidized by G6P dehydrogenase to gluconate-6-phosphate. The latter step involves concomitant reduction of cofactor NADP⁺ to NADPH, which can be spectrophotometrically measured by the increase of absorbance at 340 nm. The assays were performed in clear, flat-bottom 96-

well microplates according to the kit instructions with minor modifications: porcine trehalase (rather than the unidentified trehalase from the kit) was used at a final concentration of ~ 4 $\mu\text{g/mL}$, trehalose was used at a final concentration of 2.5 mM, trehalose analogues were used at varying concentrations, and the reaction incubation step was performed at 37 °C for 1 h. Linearity of the assay under these conditions was confirmed. Blanks lacking both trehalose and trehalose analogues were included to obtain baseline absorbance measurements. Controls lacking trehalose analogues but containing 2.5 mM trehalose were included in each analysis. Controls lacking trehalose but containing trehalose analogues at varying concentrations were included in each analysis to confirm that the analogues were not contributing to absorbance (consistent with Figure 2A showing that the analogues were not detectably hydrolyzed by porcine trehalase). Following the incubation period, absorbance at 340 nm was measured using a Tecan plate reader (Infinite F200 or M200 PRO operated by Tecan iControl software). The data were normalized and analyzed using GraphPad Prism software version 6 with an equation for dose vs. response $\log[\text{inhibitor}]$ vs. normalized response (variable slope function). Each data point corresponds to the average of triplicates \pm standard deviation per concentration of trehalose analogue. Data shown are representative of at least 2 independent trials.

***C. difficile* strains and growth assays.** *C. difficile* strains used were CD2015 (RT027), CD1015 (RT078), CD2048 (RT053),⁸ VPI10463 (RT003), and R20291 Δ treA (RT027 with clean deletion of trehalase gene).⁹ Growth studies were performed at 37°C under anaerobic conditions (5% hydrogen, 90% nitrogen, 5% carbon dioxide). Individual bacterial colonies were picked from BHIS (BHI media (Difco) supplemented with 0.5% (w/v) yeast extract) plates inoculated into BHIS liquid media, and cultured overnight. Following ~ 16 hours growth, strains were subcultured 1:40 in defined minimal media (DMM) as described previously,¹⁰ supplemented with 20 mM glucose and allowed to grow to mid log phase (~ 4 hours). Cultures were further diluted 1:40 into DMM supplemented in either trehalose, glucose, trehalose analogues, or Validamycin A (Research Products International) as indicated. Growth was assessed by averaging the OD₆₀₀ of technical replicates in a 96-well micro-titer plate every 10 minutes for 17 hours. Biological replicates were assessed in at least 3 separate experiments.

5-Thiotrehalose cytotoxicity assay. Cytotoxicity of 5-thiotrehalose in human embryonic kidney (HEK) 293 cells was assessed using a commercially available lactate dehydrogenase (LDH) release assay kit (Pierce). Briefly, 10^4 HEK 293 cells in 100 μL in of HEK cell culture medium in a 96-well tissue culture plate in triplicate were treated with varying concentrations of 5-thiotrehalose (2.5, 5.0, or 10 mM) or left untreated for positive and negative controls. Media-only blanks were also included in the plate. Cells were incubated for 48 h at 37 °C with 5% CO₂. To one triplicate set of untreated cells, 10 μL of 10X lysis buffer

were added as the positive control (maximum LDH activity), and the plate was incubated for an additional 45 min. 50 μ L of supernatant from each well were then transferred to a flat-bottom 96-well plate. To each well, 50 μ L of kit “Reaction Mixture” was added and the plate was incubated for 30 min in the dark. 50 μ L of kit “Stop Solution” was added then absorbance at 490 nm and 680 nm was measured using a microplate reader (Molecular Devices SpectraMax M3 running SoftMax Pro 6.2.2 software). From these values, percent cytotoxicity was calculated according to the kit instructions. Data reported (Table S2) are from three replicates and standard deviations are given.

III. References

- 1 I. Tvaroška, M. Hricovíni and E. Petráková, *Carbohydr. Res.*, 1989, **189**, 359–362.
- 2 S. R. Rundell, Z. L. Wagar, L. M. Meints, C. D. Olson, M. K. O’Neill, B. F. Piligian, A. W. Poston, R. J. Hood, P. J. Woodruff and B. M. Swarts, *Org. Biomol. Chem.*, 2016, **14**, 8598–8609.
- 3 L. M. Meints, A. W. Poston, B. F. Piligian, C. D. Olson, K. S. Badger, P. J. Woodruff and B. M. Swarts, *J. Vis. Exp.*, 2017, e54485.
- 4 J. M. Wolber, B. L. Urbanek, L. M. Meints, B. F. Piligian, I. C. Lopez-Casillas, K. M. Zochowski, P. J. Woodruff and B. M. Swarts, *Carbohydr. Res.*, 2017, **450**, 60–66.
- 5 R. W. Bassily, R. I. El-Sokkary, B. A. Silwanis, A. S. Nematalla and M. A. Nashed, *Carbohydr. Res.*, 1993, **239**, 197–207.
- 6 V. V Krishnamurthy, *J. Magn. Reson. A*, 1996, **121**, 33–41.
- 7 N. L. Allinger, Y. H. Yuh and J. H. Lii, *J. Am. Chem. Soc.*, 1989, **111**, 8551–8566.
- 8 C. D. Robinson, J. M. Auchtung, J. Collins and R. A. Britton, *Infect. Immun.*, 2014, **82**, 2815–2825.
- 9 J. Collins, C. Robinson, H. Danhof, C. W. Knetsch, H. C. van Leeuwen, T. D. Lawley, J. M. Auchtung and R. A. Britton, *Nature*, 2018, **553**, 291–294.
- 10 C. M. Theriot, M. J. Koenigsknecht, P. E. J. Carlson, G. E. Hatton, A. M. Nelson, B. Li, G. B. Huffnagle, J. Z Li and V. B. Young, *Nat. Commun.*, 2014, **5**, 3114.